

EFFECT OF HOT BARYONS ON THE WEAK-LENSING SHEAR POWER SPECTRUM

HU ZHAN AND LLOYD KNOX

Department of Physics, University of California, Davis, CA 95616

Draft version June 13, 2019

ABSTRACT

We investigate the impact of the intracluster medium on the weak-lensing shear power spectrum. The shear power spectrum depends on the total mass power spectrum. With the halo model, we find that the baryon power spectrum is significantly lower than the dark matter power spectrum on scales well below the linear scale. The effect on the shear power spectrum is much less pronounced. Nevertheless, the difference is on the order of a few percent for $l \gtrsim 1000$, depending on the baryon profile and source redshift. In addition, cooling/cooled baryons and the intergalactic medium can further alter the shear power spectrum. Therefore, the small-scale baryon effect should be taken into account in order to interpret future weak lensing data for precision cosmology with high multipoles.

Subject headings: cosmology: theory — dark matter — galaxies: clusters: general — gravitational lensing — large-scale structure of universe

1. INTRODUCTION

Weak gravitational lensing is a promising technique for precision cosmology. Its chief advantage over other techniques comes from its sensitivity to the total density field, rather than just the baryonic component. Since the total density is mostly due to the dark matter, which only interacts gravitationally, the statistical properties of the total density field can be calculated *ab initio* with much higher accuracy than can observables that are more directly dependent on baryons. Combined with the enormous statistical power of proposed survey projects, such as the *Large Synoptic Survey Telescope*¹ and *Supernova/Acceleration Probe*², weak lensing is thought to be capable of determining (some) cosmological parameters to a few percent level (e.g. Refregier et al. 2004).

Many studies of weak lensing statistics assume for convenience that baryons are distributed in the same way as dark matter (e.g. Bacon, Refregier & Ellis 2000; Cooray, Hu & Miralda-Escudé 2000; Hu & White 2001; Song & Knox 2003). This allows one to predict, for example, the weak-lensing shear power spectrum (PS) from the nonlinear dark matter PS that is well calibrated using *N*-body simulations (Peacock & Dodds 1996; Ma & Fry 2000; Smith et al. 2003).

However, more than 10% of the total mass is in baryons, which do not follow dark matter exactly on small scales (Gnedin & Hui 1998; Zhan 2004). Therefore the total mass distribution and its PS will deviate somewhat from those in a universe that has the same initial conditions except that all the mass is in dark matter.³ Such a deviation in the mass PS will result in a difference in weak lensing statistics. Eventually, it will be necessary to account for the baryonic influence on the shear PS as we reach for the projected statistical power

of weak lensing surveys.

Baryons exist mainly in three categories: (1) cooling/cooled baryons such as in stars and galaxies, (2) hot baryons or the intracluster medium (ICM, including the intragroup medium), and (3) the intergalactic medium (IGM). The cooling/cooled baryons can alter the statistics of gravitational lensing (White 2004), because they are able to condense to a much denser state than dark matter, which in turn modifies the dark matter distribution as well (Kazantzidis et al. 2004). The ICM is smoother than cooling/cooled baryons, so that the effect might be much less pronounced (White 2004). However, the X-ray emitting gas in a cluster greatly out-weighs the baryons in the galaxies. Therefore, the ICM could still have a significant impact on the shear PS. Indeed, we find at $l \lesssim 3000$, the ICM has a larger impact on the shear PS than do the cooling/cooled baryons.

For completeness we also note here that the IGM is much more diffuse than the other two and harder to model analytically on small scales, but it is the largest reservoir of baryons. Since the density fluctuations on the angular scales we consider are dominated by high-density and massive objects, we neglect the IGM for the present, but plan to study the IGM effect using hydrodynamical simulations in the future.

In this *Letter* we demonstrate the effect of hot baryons on the weak-lensing shear PS. Assuming an isothermal β -model (Cavaliere & Fusco-Femiano 1976) for the ICM density profile, we are able to extend the halo model (for a review, see Cooray & Sheth 2002) to include hot baryons in the total mass PS, which is then used to calculate the shear PS. This method does not give us an accurate total mass PS, because we have not included the IGM and cooling/cooled baryons and because we have made simple associations of the ICM profile with its dark matter halo. As such, the β -model and halo model together are not sufficiently accurate for interpreting future data. Nevertheless, they provide a framework for analytically estimating the effect of uncertainty in the clustering properties of hot baryons.

Electronic address: zhan@physics.ucdavis.edu

Electronic address: lknox@physics.ucdavis.edu

¹ <http://www.lsst.org/>

² <http://snap.lbl.gov/>

³ One may think of this as an *N*-body simulation of dark matter that has the same parameters and initial mass PS (including baryonic features such as due to acoustic oscillations) as a full hydrodynamical simulation.

2. MASS POWER SPECTRUM

Despite the controversy on the inner slope, realistic halo profiles (e.g. Navarro, Frenk & White 1996; Moore et al. 1999) have enabled the halo model to reproduce the nonlinear dark matter PS. The halo model decomposes the dark matter PS into multiple halo components. With the one-halo PS $P_{\text{dm}}^{\text{1h}}(k)$ and two-halo PS $P_{\text{dm}}^{\text{2h}}(k)$, the dark matter PS $P_{\text{dm}}(k)$ can be approximated by (Peacock & Smith 2000; Ma & Fry 2000; Seljak 2000; Scoccimarro et al. 2001)

$$P_{\text{dm}}(k) = P_{\text{dm}}^{\text{1h}}(k) + P_{\text{dm}}^{\text{2h}}(k), \quad (1)$$

$$P_{\text{dm}}^{\text{1h}}(k) = \int f(\nu) d\nu \frac{m_{\text{d}}(\nu)}{\bar{\rho}_{\text{d}}} |u_{\text{d}}[k, m_{\text{d}}(\nu)]|^2,$$

$$P_{\text{dm}}^{\text{2h}}(k) = P_{\text{L}}(k) \left\{ \int f(\nu) b(\nu) d\nu u_{\text{d}}[k, m_{\text{d}}(\nu)] \right\}^2,$$

where $\bar{\rho}_{\text{d}}$ is the mean density of the universe at the present, $u_{\text{d}}[k, m_{\text{d}}(\nu)]$ is the normalized profile of a dark matter halo with mass m_{d} in Fourier space (for specific forms, see Cooray & Sheth 2002), and P_{L} is the linear mass PS. Note that the dark-matter density profile is cut off at the virial radius. The height of the density peak, ν , is defined as

$$\nu = [\delta_c(z)/\sigma(m_{\text{d}})]^2, \quad (2)$$

where $\delta_c(z) \simeq 1.686\Omega_m^{0.0055}(z)$ (Hiotelis 2003) is the overdensity of a spherical region that collapses at redshift z , $\Omega_m(z)$ is the ratio of matter density to critical density at z , and $\sigma(m_{\text{d}})$ is the rms value of the density contrast $\delta\rho_{\text{d}}/\rho_{\text{d}}$ within a radius of $(3m_{\text{d}}/4\pi\bar{\rho}_{\text{d}})^{1/3}$ at z . Equation (2) also defines the function $m_{\text{d}}(\nu)$. The functions $f(\nu)$ and $b(\nu)$, related to the halo mass function and bias, respectively, have the forms (Sheth & Tormen 1999)

$$\begin{aligned} \nu f(\nu) &= A(1 + \nu_1^{-p})\nu_1^{1/2} e^{-\nu_1/2}, \\ b(\nu) &= 1 + \frac{\nu_1 - 1}{\delta_c} + \frac{2p}{\delta_c(1 + \nu_1^p)}, \end{aligned}$$

with $\nu_1 = 0.707\nu$ and $p = 0.3$. The normalization constant A satisfies the constraint $\int f(\nu) d\nu = 1$.

When hot baryons are included, equation (1) can be extended to read

$$\begin{aligned} P(k) &= \sum_{ij} f_i f_j P_{ij}(k), \quad (3) \\ P_{ij} &= P_{ij}^{\text{1h}} + P_{ij}^{\text{2h}}, \\ P_{ij}^{\text{1h}} &= \int f(\nu) d\nu \frac{m_{\text{d}}(\nu)}{\bar{\rho}_{\text{d}}} u_i[k, m_{\text{d}}(\nu)] u_j[k, m_{\text{d}}(\nu)], \\ P_{ij}^{\text{2h}} &= P_{\text{L}}(k) \int f(\nu) b(\nu) d\nu u_i[k, m_{\text{d}}(\nu)] \\ &\quad \times \int f(\nu') b(\nu') d\nu' u_j[k, m_{\text{d}}(\nu')], \end{aligned}$$

where the subscripts $i, j = \text{d}$ for dark matter and b for baryons. The coefficients, f_{d} and f_{b} , are the fractions of dark matter and baryons in total halo mass, respectively. Obviously, $P_{ij}(k) = P_{ji}(k)$, $f_{\text{d}} + f_{\text{b}} = 1$, and equation (1) is a special case of equation (3) when $f_{\text{b}} = 0$.

For Equation (3) we have assumed a fixed gas-mass fraction f_{b} . In principle, there should be a distribution of gas-mass fraction for a given halo mass, and this distribution can be halo mass dependent (or ICM

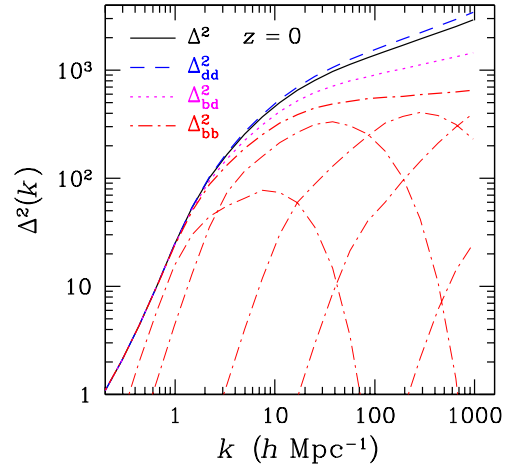


FIG. 1.— Halo-model mass power spectra at $z = 0$. The total power spectrum $\Delta^2(k)$ (solid line) is calculated using equation (3) as a weighted sum of the dark matter power spectrum $\Delta_{\text{dd}}^2(k)$ (dashed line), the baryon-dark matter cross power spectrum $\Delta_{\text{bd}}^2(k)$ (dotted line), and the baryon power spectrum $\Delta_{\text{bb}}^2(k)$ (dash-dotted line). From left to right, the thin dash-dotted lines represent one-halo contributions to the baryon power spectrum from mass ranges of $10^{17} M_{\odot} \geq m_{\text{d}} > 10^{14} M_{\odot}$, $10^{14} M_{\odot} \geq m_{\text{d}} > 10^{12} M_{\odot}$, $10^{12} M_{\odot} \geq m_{\text{d}} > 10^{10} M_{\odot}$, $10^{10} M_{\odot} \geq m_{\text{d}} > 10^7 M_{\odot}$, and $10^7 M_{\odot} \geq m_{\text{d}} \geq 10^4 M_{\odot}$.

temperature dependent, see Arnaud & Evrard 1999; Mohr, Mathiesen & Evrard 1999). Although the dependence is found to be weak for clusters (Ota & Mitsuda 2004), it may not be true for low mass systems. Hence, an average over the distribution should be incorporated numerically to calculate the PS. We assume for simplicity and convenience that f_{b} equals the cosmic mean baryon fraction of 0.13.

The Fourier-space baryon profile $u_{\text{b}}[k, m_{\text{d}}(\nu)]$ is calculated from the isothermal β -model, i.e.

$$\rho_{\text{b}}(r) = \rho_{\text{b}0} \left(1 + \frac{r^2}{r_c^2} \right)^{-3\beta/2},$$

where $\rho_{\text{b}0}$ is the central baryon density, r_c the core radius, and $\beta = 0.4\text{--}1.2$ (Mohr, Mathiesen & Evrard 1999; Mulchaey et al. 2003; Ettori et al. 2004; Ota & Mitsuda 2004). The baryon profile is also cut off at the virial radius. Assuming hydrostatic equilibrium and the NFW halo profile (Navarro, Frenk & White 1996), Makino, Sasaki & Suto (1998) find that the best-fitting β -model has a core radius about one-fifth of the scale radius, r_s , of the NFW profile. We choose $\beta = 0.7$ and $r_c = 0.22r_s$ to be the fiducial model and allow the parameters to vary.

Fig. 1 shows the fiducial model PS at $z = 0$ in dimensionless form, i.e. $\Delta^2(k) = k^3 P(k)/2\pi^2$. We have assumed a flat universe with $\Omega_m = 0.3$, $\Gamma = 0.18$, $\sigma_8 = 0.85$, and $n = 1$, where Γ is the shape parameter of the PS, σ_8 is the rms value of the density contrast within a radius of $8 h^{-1}\text{Mpc}$, and n is the power spectral index. Since, for the fiducial model, the baryon density profile is smoother than the dark matter density profile (for examples, see Makino, Sasaki & Suto 1998), the baryon PS $\Delta_{\text{bb}}^2(k)$ and baryon-dark matter cross PS $\Delta_{\text{bd}}^2(k)$ should be lower than the dark matter PS $\Delta_{\text{dd}}^2(k)$ on small scales where the one-halo term dominates. As

expected, $\Delta_{\text{bb}}^2(k)$ and $\Delta_{\text{bd}}^2(k)$ become significantly lower than $\Delta_{\text{dd}}^2(k)$ at $k > 1 h \text{ Mpc}^{-1}$. At higher redshift, this departure occurs at a larger wavenumber. Consequently, the total mass PS is lower than what it would be if the hot baryons are replaced by dark matter.

From the break-down of the contributions to the one-halo baryon PS, also shown in Fig. 1, one sees that each group of halos dominates a certain range of scales. We have included very low mass ($m_{\text{d}} < 10^{10} M_{\odot}$) halos in our calculations. The β -model does not necessarily apply to these low mass systems, but since they contribute very little to the mass PS at $k < 100 h \text{ Mpc}^{-1}$ – the most important scales to shear PS at l less than a few thousand – our conclusions will not be affected.

3. SHEAR POWER SPECTRUM

With the Limber approximation and the assumption that sources are on a thin slice at z , the shear PS C_l in a flat universe is given by (Bacon, Refregier & Ellis 2000; Hu 2000; Bartelmann & Schneider 2001)

$$C_l = \frac{9}{4} \left(\frac{H_0}{c} \right)^4 \left(\frac{\Omega_m}{D_s} \right)^2 \int_0^{D_s} dD \left(\frac{D_s - D}{a} \right)^2 P(k; z), \quad (4)$$

where H_0 is the Hubble constant at $z = 0$, c is the speed of light, D and D_s are the comoving distance of the lens and sources, respectively, $a = (1 + z)^{-1}$, and $k = l/D$. We define $\mathcal{C}_l \equiv 2C_l/\pi$, which is the contribution to the variance of the deflection angle from logarithmic intervals in l . The results are shown in Fig. 2 for the fiducial model. Since the shear PS is mostly affected by the linear and quasi-linear part of the mass PS, the effect of hot baryons on the shear PS is less than a few percent for $l \lesssim 3000$. As redshift increases, the same l corresponds to smaller wavenumbers (large scales), meanwhile the PS is more linear at the same wavenumber. In addition, hot baryons make less of a difference in the mass PS at higher redshift. Thus, the effect of the ICM on the shear PS reduces with increasing redshift.

The effect of the ICM on the shear PS is large enough that it will need to be addressed if the cosmological parameter errors forecasted in, e.g., Song & Knox (2003, with $l_{\text{max}} = 1000$), Hu (2002, with $l_{\text{max}} = 3000$) and Refregier et al. (2004, with $l_{\text{max}} = 2 \times 10^5$) are to be realized. This is clear from the lower panel of Fig. 2 where departures outside the shaded region are larger than the statistical error for a fiducial survey with parameter values as given in the caption. The statistical error in \mathcal{C}_l in a band of width $l/4$ is given by

$$\Delta \mathcal{C}_l = 0.004 \left(\frac{1000}{l} \right) \left(\frac{0.25}{f_{\text{sky}}} \right)^{1/2} \left(\mathcal{C}_l + \frac{2}{\pi} \frac{\gamma_{\text{rms}}^2}{\bar{n}} \right), \quad (5)$$

where f_{sky} is the fraction of sky covered, \bar{n} is the number density of sources with measurable shapes, and γ_{rms}^2 is the variance of the “shape noise”.

From the break-down of the contributions from different mass halos, one sees that the two-halo term in the mass PS, or effectively the linear mass PS, is the largest contributor at large angular scales (small l ’s), and only those massive halos ($m_{\text{d}} > 10^{12} M_{\odot}$) are important to the shear PS at small angular scales.

Observationally, the β parameter and the core radius assume a range of values. In fact, the baryon profile

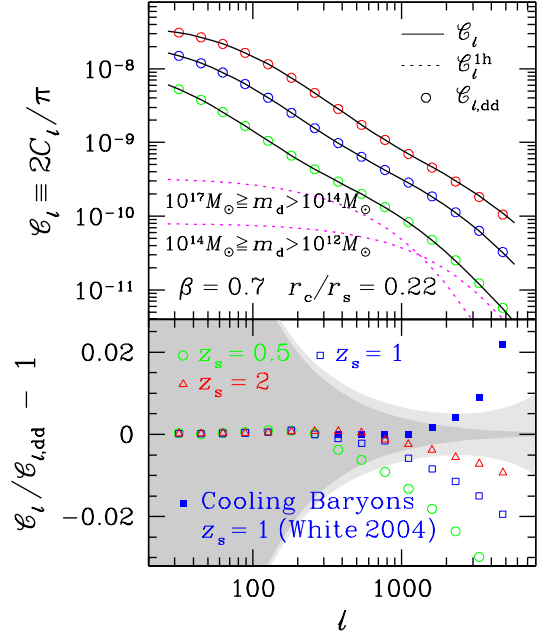


FIG. 2.— The upper panel illustrates shear power spectra with and without baryons (solid lines and circles, respectively). From bottom to top, the solid lines and circles assume sources to be on a thin slice at $z = 0.5, 1$, and 2 . The dotted lines represent one-halo contributions to the total shear power spectrum \mathcal{C}_l at $z = 0.5$. Contributions from halos with mass less than $10^{12} M_{\odot}$ are below 10^{-12} . The fractional difference are shown in the lower panel. The dark grey band is the one σ statistical error on a band of width $l/4$ in the sample variance limit for a survey with $f_{\text{sky}} = 0.25$. The light grey band includes shape noise for the $z_s = 1$ power spectrum assuming $\bar{n} = 10/\text{arcmin}^2$ and $\gamma_{\text{rms}} = 0.2$.

becomes more compact than the dark matter profile if β is larger and the core-radius-to-scale-radius ratio is smaller. This can drive the baryon-dark matter cross PS and baryon PS higher than the dark matter PS, and results in an increase in the shear PS. On the other hand, the entropy floor (Ponman, Cannon & Navarro 1999) can increase the core radius of the baryon profile in low mass systems (Tozzi & Norman 2001; Holder & Carlstrom 2001) and reduce the total mass PS and shear PS.

Fig. 3 explores the relative changes in the shear PS in the $\beta-r_c/r_s$ space for $l = 1000$ and 3000 . We see that given the observational uncertainties about the β -model parameters, hot baryons could pose a significant challenge to precision cosmology.

We are optimistic that the challenge can be met, at least for $l \lesssim 3000$, by a combination of hydrodynamic numerical calculations, and observations of hot gas via X-ray emission and the SZ effect. Fortunately, it is only very massive halos that are important at $l \lesssim 3000$, and these are just the ones easiest to study in X-ray and SZ. Planned SZ surveys such as SPT, ACT, APEX and SZA will have sufficient angular resolution and observe a sufficiently large number of clusters to guide the development of a statistical model of ICM profiles. Observing strategy can also, to some degree, mitigate the difficulties posed by baryons. Their importance at small scales argue for large sky coverage, to reduce sample variance (thereby improving the \mathcal{C}_l measurement on all scales), rather than depth and angular resolution, which reduce the shape

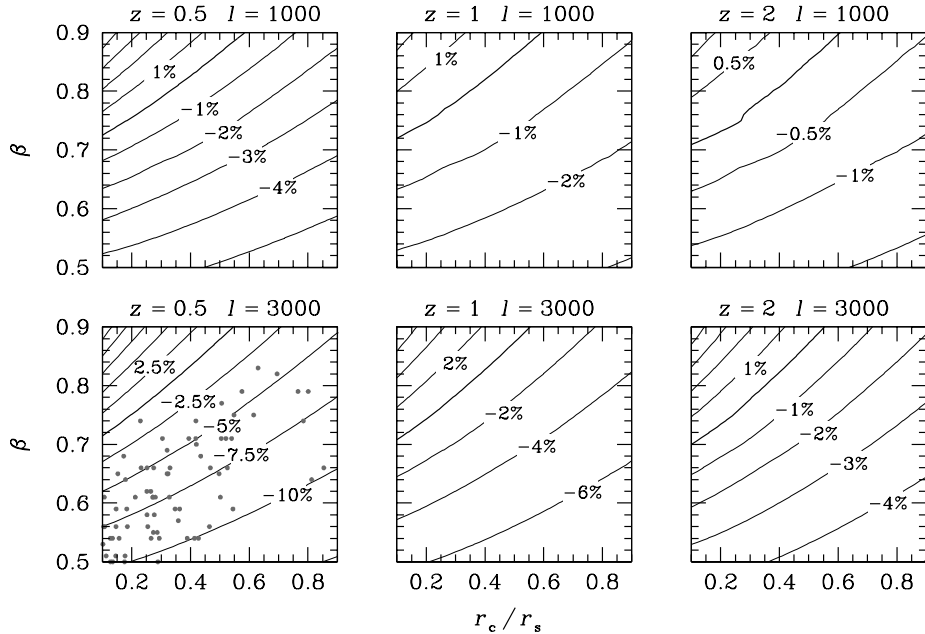


FIG. 3.— Contours of the fractional difference, $\mathcal{C}_l / \mathcal{C}_{l,dd} - 1$, in $\beta - r_c / r_s$ space. Grey dots in the lower left panel correspond to the observed values of β and r_c / r_s from Mohr, Mathiesen & Evrard (1999) and Ota & Mitsuda (2004).

noise that is only important at small scales.

4. DISCUSSION AND CONCLUSIONS

We have extended the halo model to calculate the total mass PS of dark matter and hot baryons. Given the observed properties of the ICM, we find the total mass PS is considerably lower than the dark matter PS on scales approximately an order of magnitude below the nonlinear scale. This leads to a few percent reduction of the shear PS at $1000 \lesssim l \lesssim 3000$ compared to what it would be if baryons traced dark matter exactly. The effect grows with increasing l . Further, for $l \gtrsim 3000$ an effect (with opposite sign, see Fig. 2) also becomes important due to cooling/cooled baryons (White 2004).

So far, we have not considered the IGM (including the warm-hot IGM, Davé et al. 2001), which contains roughly two thirds of the baryons at $z = 0$. This fraction becomes larger at higher redshift. Using hydrodynamical simulations (TreeSPH, Davé, Dubinski & Hernquist

1997) that incorporate cooling, heating, star formation, and feedback, Zhan (2004) obtains a total baryon PS that is lower than what has been shown in Fig. 1. Therefore, when all the baryons are accounted for, the effect on weak lensing statistics could be even greater. A detailed investigation using hydrodynamical simulations will be necessary to assess the total baryon effect quantitatively. In conclusion, for precision cosmology with weak lensing to live up to its promise, we will have to pay attention to the modeling of baryons, and not just the dark matter.

We thank A. Stebbins for a useful conversation and J. A. Tyson for commenting on the manuscript. HZ also thanks C. Fassnacht and L. Lubin for discussions on the ICM profile. This work was supported by the National Science Foundation under Grant No. 0307961 and NASA under grant No. NAG5-11098.

REFERENCES

Arnaud, M., & Evrard, A. E. 1999, MNRAS, 305, 631
 Bacon, D. J., Refregier, A. R., & Ellis, R. S. 2000, MNRAS, 318, 625
 Bartelmann, M., & Schneider, P. 2001, Phys. Rep., 340, 291
 Cavaliere, A., & Fusco-Femiano, R. 1976, A&A, 49, 137
 Cooray, A., Hu, W., & Miralda-Escudé, J. 2000, ApJ, 535, L9
 Cooray, A., & Sheth, R. 2002, Phys. Rep., 372, 1
 Davé, R. et al. 2001, ApJ, 552, 473
 Davé, R., Dubinski, J., & Hernquist, L. 1997, New Astro., 2, 277
 Ettori, S., Tozzi, P., Borgani, S., & Rosati, P. 2004, A&A, 417, 13
 Hiotelis, N. 2003, MNRAS, 344, 149
 Holder, G. P., & Carlstrom, J. E. 2001, ApJ, 558, 515
 Hu, W. 2000, Phys. Rev. D, 62, 043007
 Hu, W. 2002, Phys. Rev. D, 65, 23003
 Hu, W., & White, M. 2001, ApJ, 554, 67
 Kazantzidis, S., Kravtsov, A. V., Zentner, A. R., Allgood, B., Nagai, D., & Moore, B. 2004, ApJ, 611, L73
 Ma, C.-P., & Fry, J. N. 2000, ApJ, 543, 503
 Makino, N., Sasaki, S., & Suto, Y. 1998, ApJ, 497, 555
 Mohr, J. J., Mathiesen, B., & Evrard, A. E. 1999, ApJ, 517, 627
 Moore, B., Quinn, T., Governato, F., Stadel, J., & Lake, G. 1999, MNRAS, 310, 1147
 Mulchaey, J. S., Davis, D. S., Mushotzky, R. F., & Burstein, D. 2003, ApJS, 145, 39
 Navarro, J. F., Frenk, C. S., & White, S. D. M. 1996, ApJ, 462, 563
 Nedin, N. Y., & Hui, L. 1998, MNRAS, 296, 44
 Ota, N., & Mitsuda, K. 2004, A&A, in press, astro-ph/0407602
 Peacock, J. A., & Dodds, S. J. 1996, MNRAS, 280, L19
 Peacock, J. A., & Smith, R. E. 2000, MNRAS, 318, 1144
 Ponman, T. J., Cannon, D. B., & Navarro, J. F. 1999, Nature, 397, 135
 Refregier, A. et al. 2004, AJ, 127, 3102
 Scoccimarro, R., Sheth, R. K., Hui, L., & Jain, B. 2001, ApJ, 546, 20
 Seljak, U. 2000, MNRAS, 318, 203
 Sheth, R. K., & Tormen, G. 1999, MNRAS, 308, 119
 Smith, R. E. et al. 2003, MNRAS, 341, 1311

Song, Y., & Knox, L. 2003, Phys. Rev. D, 68, 043518
Tozzi, P., & Norman, C. 2001, ApJ, 546, 63
White, M. 2004, Astroparticle Phys., in press, astro-ph/0405593

Zhan, H. 2004, PhD Thesis, Univ. of Arizona, astro-ph/0408379